Solid State Phenomena
ISSN: 1662-9779, Vol. 390, pp 189-195
doi:10.4028/p-bdcs2V

Submitted: 2026-01-19
Revised: 2026-02-24
Accepted: 2026-02-25
Online: 2026-04-17

Further Developments of Hill-Gotoh Theory of Anisotropic Sheet Metal Plasticity

Wei TONG[1,a*]

[1]Department of Mechanical Engineering, Southern Methodist University, Dallas, Texas USA

[a] wtong@smu.edu (*corresponding author)

Keywords: non-quadratic yield criteria, non-homogeneous stress functions, convexity.

Abstract. An associated plasticity theory of combining Hill's 1948 quadratic and Gotoh's 1977 quartic stress functions [1,2] has recently been developed for modeling orthotropic steel sheet metals in plane stress [3]. Some further developments of the theory with a higher-order non-homogenous polynomial yield stress function are described in this study. Numerical examples are given to illustrate the expanded capabilities for modeling thin steel sheet metals in plane stress by the enhanced Hill-Gotoh anisotropic plasticity theory.

Introduction

Modern mathematical modeling of the yielding and plastic flow of anisotropic sheet metals has been developed following the initial framework as outlined by Hill in his 1950 plasticity monograph [4]. Many current widely used advanced theories of macroscopic anisotropic plasticity replace Hill's 1948 quadratic yield stress function with one of non-quadratic yield stress functions such as Yld2000-2d and Yld2004-18p [5,6]. When only even-order stress exponents such as 6 or 8 are adapted, those non-quadratic yield stress functions are in fact simply higher-order homogenous polynomials of Cauchy stress with many more polynomial coefficients.

To extend the modeling capabilities of either Hill's 1948 quadratic theory [1] or Gotoh's 1977 quartic theory [2], an anisotropic yield stress function has recently been proposed as a sum of both quadratic and quartic stress functions [3]. The new yield stress function is a single fourth-order non-homogeneous polynomial with 13 even-order stress terms and associated coefficients. The initial application results of the proposed fourth-order theory to model anisotropic yielding and plastic flow of four steel sheets have been encouraging. Further developments of the theory are presented in the following, namely, the generalized formulation of higher-order non-homogeneous polynomial yield functions based on Hill's quadratic and Gotoh's quartic stress functions and the use of a novel least-square parameter identification method with a set of heuristic matrix-based convexity constraints.

The generalized Hill-Gotoh theory

The quadratic and quartic yield functions in the classical Hill's 1948 theory [1] and in Gotoh's 1977 fourth-order theory are of the following forms (for plane stress)

$$\Phi_h = A_1\sigma_x^2 + A_2\sigma_x\sigma_y + A_3\sigma_y^2 + A_4\tau_{xy}^2, \tag{1}$$

$$\Phi_g = B_1\sigma_x^4 + B_2\sigma_x^3\sigma_y + B_3\sigma_x^2\sigma_y^2 + B_4\sigma_x\sigma_y^3 + B_5\sigma_y^4 + \left(B_6\sigma_x^2 + B_7\sigma_x\sigma_y + B_8\sigma_y^2\right)\tau_{xy}^2 + B_9\tau_{xy}^4, \tag{2}$$

with a total of 4 and 9 polynomial coefficients respectively. A generalized Hill-Gotoh yield function is proposed in terms of the normalized Cauchy stress $\overline{\boldsymbol{\sigma}} = \left(\sigma_x, \sigma_y, \tau_{xy}\right)/\sigma_f$ as

$$\Phi_{hg}(\overline{\boldsymbol{\sigma}}) = \Phi_h^{M_1}(\overline{\boldsymbol{\sigma}}) + \Phi_g^{M_2}(\overline{\boldsymbol{\sigma}}) + \Phi_h^{M_3}(\overline{\boldsymbol{\sigma}}) + \Phi_g^{M_4}(\overline{\boldsymbol{\sigma}}) + \ \ldots, \tag{3}$$

where $(M_1, M_2, M_3, M_4, \ldots)$ are positive integers. If $(M_1, M_2) = (1,1)$, the original fourth-order Hill-Gotoh yield function with 13 coefficients as proposed in [3] is recovered. A higher-order Hill-Gotoh yield function with 17 coefficients would have non-zero (M_1, M_2, M_3), including the second Hill function $\Phi_h^{M_3}(\overline{\boldsymbol{\sigma}})$ of degree $2M_3$ with additional four parameters (C_1, C_2, C_3, C_4).

Convexity-constrained least square parameter identification

It is well-known that a polynomial stress function (homogeneous or otherwise) is in general not guaranteed to be positive and convex and thus may not be automatically used as a valid yield function [5-7]. For example, using eight inputs from uniaxial and biaxial tension tests on an IF steel from [8] and a packaging steel from [9], one can obtain eight on-axis polynomial coefficients of the fourth-order Hill-Gotoh yield function with $(M_1, M_2) = (1,1)$ by solving eight linearly independent equations or a simple least square parameter identification problem without any convexity constraints as described in [3]. Both the experimental inputs with and as-calibrated model parameters for the two steel sheets are listed in Table 1 and Table 2 respectively.

Table 1. Material property data [8] and non-convex Hill-Gotoh parameters for an IF steel

σ_0/σ_f	r_0	σ_{90}/σ_f	r_{90}	σ_b/σ_f	r_b	σ_{p0}/σ_f	σ_{p90}/σ_f
1	1.85	0.993	2.51	1.152	0.777	1.242	1. 247
A_1	A_2	A_3	B_1	B_2	B_3	B_4	B_5
2.04046	-2.56993	2. 03626	-1.04046	2.62238	-3.73080	2.61784	-1.03657

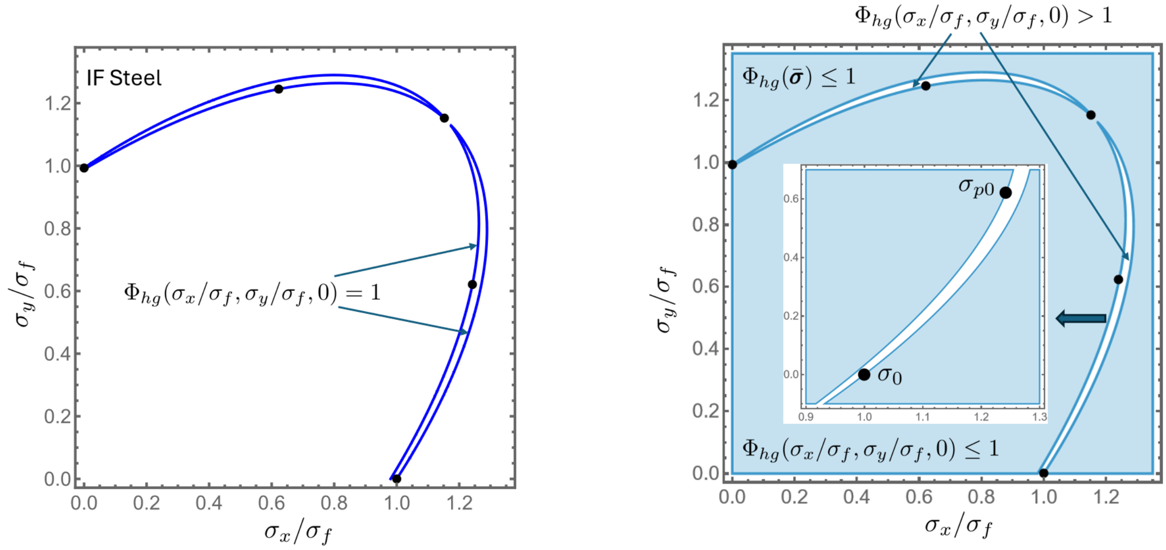

(a) (b)

Fig. 1. Predicted non-convex on-axis biaxial yield surface contours (a) and elastic-plastic domains as filled regions (b) by the fourth-order Hill–Gotoh yield function for an IF steel without SOS-convexity constraints. Solid circles are experimental yield stresses in RD and TD directions.

As shown in Fig.1(a) and Fig.2(a), the resulting biaxial fourth-order yield surfaces $\Phi_{hg}(\bar{\boldsymbol{\sigma}}) = 1$ have multiple branches and are non-convex for both steel sheets. The non-convexity of both yield surfaces can be better visualized via Fig.1(b) and Fig.2(b) respectively. For the IF steel shown in Fig.1(b), the non-accessible (unfilled) region $\Phi_{hg}(\bar{\boldsymbol{\sigma}}) > 1$ is between two elastic-plastic domains (the filled or shaded regions) $\Phi_{hg}(\bar{\boldsymbol{\sigma}}) \leq 1$. As indicated by the insert in Fig.1(b), the yield stress σ_0 under uniaxial tension along the rolling direction (RD) is on the second or outer contour. Its outer surface normal is pointed inward, so the associated elastic-plastic domain or its yield surface is thus non-convex. For the packaging steel shown in Fig.2(b), the inner elastic-plastic domain (the filled or shaded region in the middle) $\Phi_{hg}(\bar{\boldsymbol{\sigma}}) \leq 1$ is clearly non-convex between yield stresses (σ_0, σ_{p0}). Although they predict perfectly the eight experimental inputs listed in Table 1 and Table 2, these non-convex Hill-Gotoh plane-stress functions cannot be used as suitable yield functions in numerical analyses of sheet metal forming of these two steels.

Table 2. Material property data [9] and non-convex Hill-Gotoh parameters for a packaging steel

σ_0/σ_f	r_0	σ_{90}/σ_f	r_{90}	σ_b/σ_f	r_b	σ_{p0}/σ_f	σ_{p90}/σ_f
1	0.8352	1.0826	1.5097	1.0910	0.5533	1.1194	1.3024
A_1	A_2	A_3	B_1	B_2	B_3	B_4	B_5
1.92368	-0.898249	0.385033	-0.923678	0.828781	-0.193689	-0.590039	0.399474

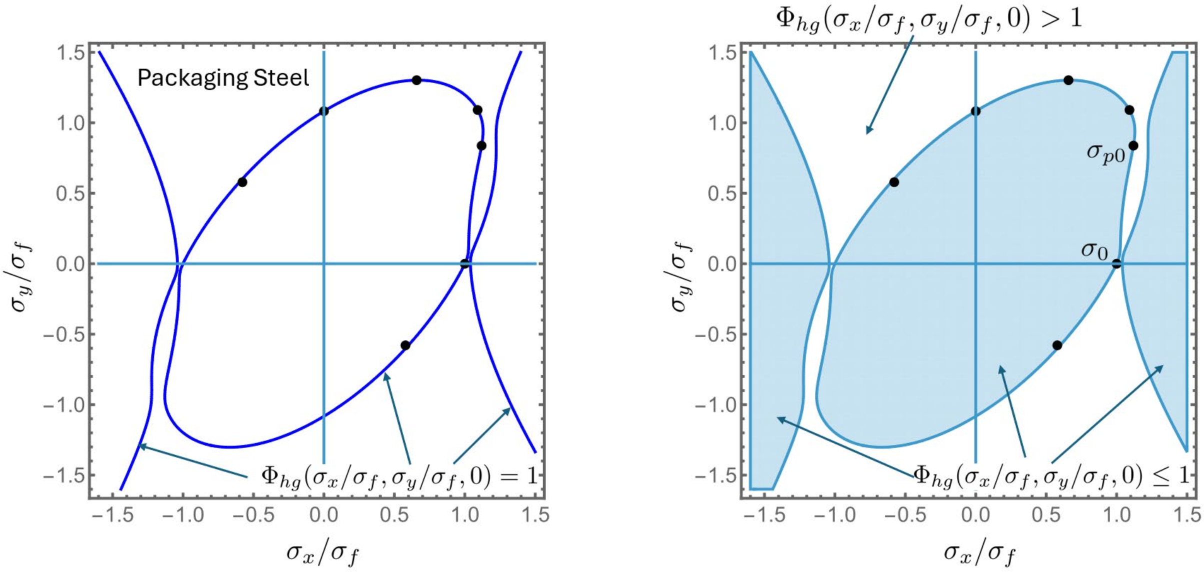

(a) (b)

Fig. 2. Predicted non-convex on-axis biaxial yield surface contours (a) and elastic-plastic domains as filled regions (b) by the Hill–Gotoh yield function for a packaging steel without SOS-convexity constraints. Solid circles are experimental yield stresses at RD and TD directions.

On the other hand, the least square minimization of yield and flow conditions with sum-of squares (SOS) convexity constraints as proposed in [3] will produce a set of 8 on-axis polynomial coefficients listed as cases (1) and (3) in Table 3 for IF and packaging steels, resulting in a strictly convex fourth-order Hill-Gotoh yield function. The SOS-convexity is only a sufficient condition of convexity for the yield surface [7] and may be too restrictive to give the resulting yield function with high accuracy. Alternatively, one can use a new set of heuristic matrix-based convexity constraints recently presented in [10] for the least square parameter identification of the strictly convex fourth-order Hill-Gotoh yield function. The corresponding sets of 8 on-axis polynomial coefficients are listed as cases (2) and (4) in Table 3 for both steels respectively. The novel numerical minimization algorithm detailed in Appendix B in [10] ensures that the curvature of a yield surface is positive everywhere (as this is known as the necessary and sufficient criterion for its strict convexity per [11-15]). Predicted on-axis biaxial yield surface contours by SOS-convex Hill–Gotoh yield functions are shown in Fig.3(a) for IF steel and in Fig.4(a) for a packaging steel. Similarly, predicted on-axis biaxial yield surface contours by Hill–Gotoh yield functions based on positive surface curvature constraints are shown in Fig.3(b) for IF steel and in Fig.4(b) for a packaging steel. Little differences are seen between the two yield surfaces of IF steel shown in Fig.3(a) and Fig.3(b). However, the yield surface shown in Fig.4(b) fits better the experimental yield stresses than the yield surface shown in Fig.4(a).

Table 3. Strictly convex Hill-Gotoh parameter sets for two steel sheets listed in Tables 1 and 2

A_1	A_2	A_3	B_1	B_2	B_3	B_4	B_5
(1) 0.64697	-1.45715	1.02246	0.35203	-0.29938	0.39998	-0.035531	0.013201
(2) 0.98390	-1.70649	1.25349	0.016102	0.38592	-0.55365	0.56946	-0.22761
(3) 0.97174	-0.77007	0.57856	0.02826	-0.17262	0.48497	-0.49282	0.23228
(4) 1.37938	-0.015936	-0.42313	-0.37938	-0.55396	1.94480	-2.16443	1.08642

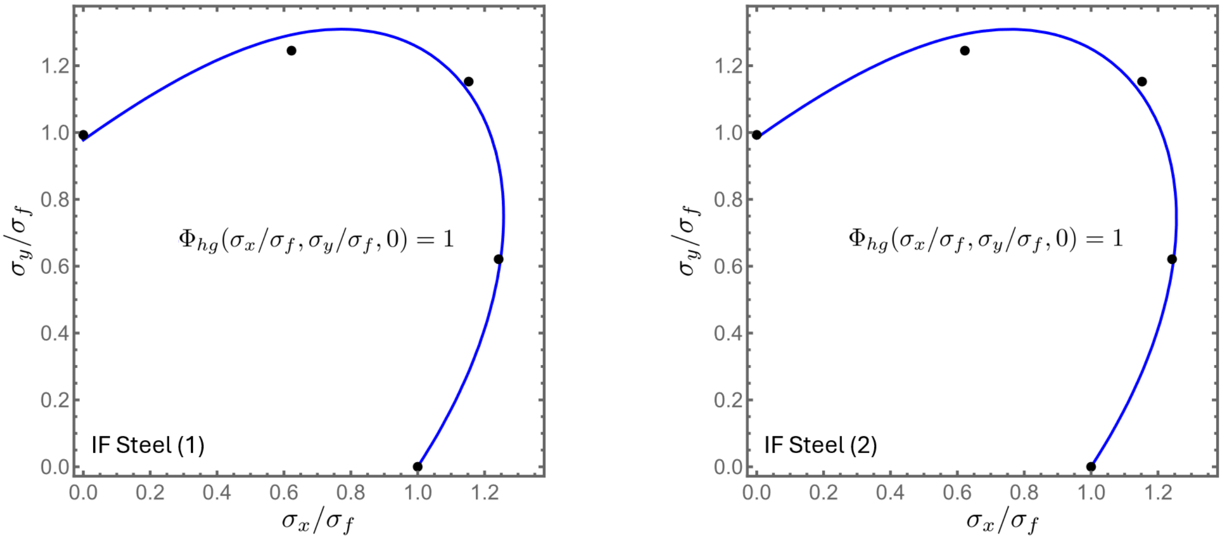

(a) (b)

Fig. 3. Predicted strictly convex on-axis biaxial yield surface contours by Hill–Gotoh yield functions (1) and (2) in Table 3 for the IF steel sheet based on SOS-convexity (a) and positive surface curvature (b) constraints [3,10].

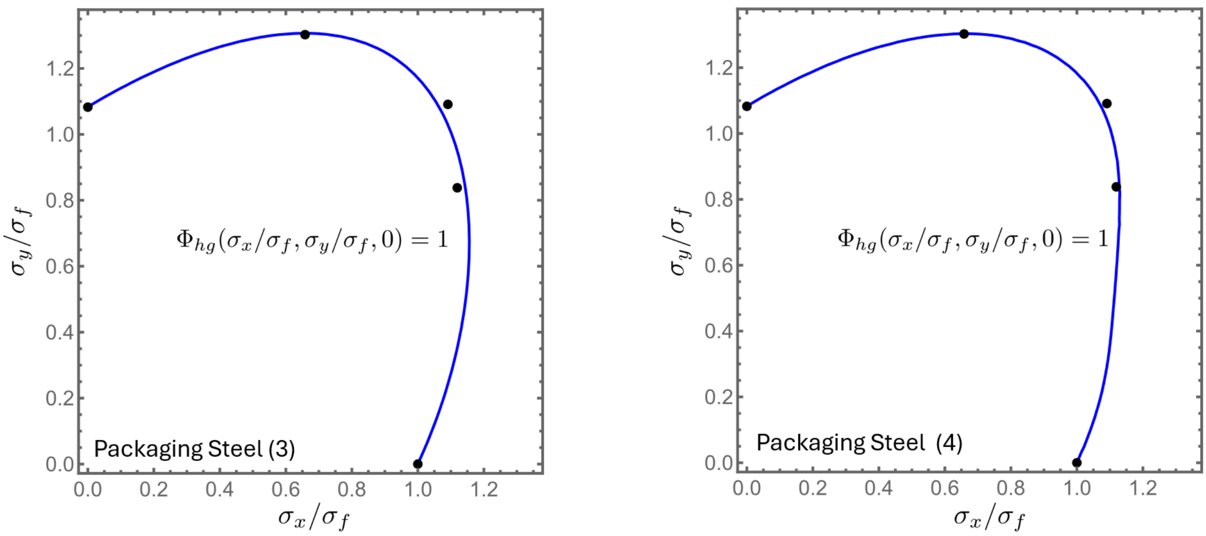

(a) (b)

Fig. 4. Predicted strictly convex on-axis biaxial yield surface contours by Hill–Gotoh yield functions (3) and (4) in Table 3 for the packaging steel sheet based on SOS-convexity (a) and positive surface curvature (b) constraints [3,10].

An Application Example of a Sixth-Order Hill-Gotoh Yield Function with 17 Parameters

One version of sixth-order non-homogeneous Hill-Gotoh yield functions may have $(M_1, M_2, M_3) = (1,1,3)$, with a total of 17 material parameters (noting that the four additional parameters are non-polynomial coefficients): (A_1, A_2, A_3, A_4), $(B_1, B_2, B_3, B_4, B_5, B_6, B_7, B_8, B_9)$ and (C_1, C_2, C_3, C_4). Using the 17 experimental and auxiliary inputs for DX54 steel sheet as listed in Table 4, one can readily obtain the values of these 17 material parameters via convexity-constrained least square parameter identification [3,10]. Table 5 lists the parameters values for the case of SOS-convexity (the first SOS rows) and for the case of positive surface curvature (the second PSC rows) respectively.

Table 4. The complete set of 17 experimental and auxiliary inputs for DX54 steel sheet [3,9]

σ_0/σ_f	r_0	σ_{90}/σ_f	r_{90}	σ_b/σ_f	r_b	σ_{p0}/σ_f	σ_{p90}/σ_f	σ_{s0}/σ_f
1	2.2157	0.9898	2.4043	1.1467	0.9507	1.2570	1.2669	0.5408
σ_{45}/σ_f	r_{45}	σ_{225}/σ_f	r_{225}	σ_{675}/σ_f	r_{675}	σ_{p45}/σ_f	σ_{s45}/σ_f	
1.0350	1.675	1. 01750	1.9454	1.0124	2.03965	1.2293	0.5588	

Using these calibrated material parameters, strictly SOS-convex on-axis and off-axis biaxial yield surface contours predicted by the sixth-order Hill–Gotoh yield function are shown as solid lines in Fig.5(a) and Fig.5(b) respectively for DX54 steel. Similarly, strictly convex on-axis and off-axis biaxial yield surface contours predicted by the sixth-order Hill–Gotoh yield function based on the positive surface curvature constraints are shown as solid lines in Fig.6(a) and Fig.6(b) respectively for DX54 steel. The on-axis yield surface shown in Fig.6(a) fits better the experimental yield stresses than the yield surface shown in Fig.5(a). Little differences are seen however between the two off-axis yield surfaces of DX54 steel sheet shown in Fig.5(b) and Fig.6(b). The corresponding uniaxial tensile yield stresses and plastic strain ratios predicted by the SOS-convex sixth-order Hill–Gotoh yield function are shown in Fig.7(a) and Fig.7(b) respectively.

Table 5. Two complete sets of 17 material parameters of the sixth-order Hill-Gotoh yield function

A_1	A_2	A_3	A_4	B_1	B_2	B_3	B_4	B_5
0.87850	-1. 26128	0.92056	3.13361	0.10883	-0.29336	0.59680	-0.30269	0.09327
1.48501	-1. 58715	1.13104	3.72566	−0.53685	0.98580	-0.84421	0.31568	−0.12136
B_6	B_7	B_8	B_9	C_1	C_2	C_3	C_4	
0.43469	-0.43791	0.38263	0.06862	0. 33553	-0.17333	0.02253	0.39824	(SOS)
−1.93345	1.43194	-0.90728	-1.81466	-0.47716	0.58038	0.17430	0.27265	(PSC)

In comparison with the visual inspection approach, the existence of a negative curvature on a yield surface via numerical computations can be used more effectively and rigorously to detect its non-convexity. Algebraic curvature formulas for implicit 2D plane curves and 3D surfaces have been summarized by Goodman [16] and for hypersurfaces in general with respect to their Hessian matrix have been discussed by Henrion and Louembet [15]. Non-convex yield surfaces shown in Fig.1 and Fig.2 are found indeed to have negative curvatures (e.g., at the uniaxial tension stresses along rolling and transverse direction for the IF steel sheet). On the other hand, the minimum curvature of yield surfaces shown in Fig.3-Fig.6 is all positive using the numerical algorithm given by Eq. (B.1) of Appendix B in [10]. Their strict convexity is thus firmly established.

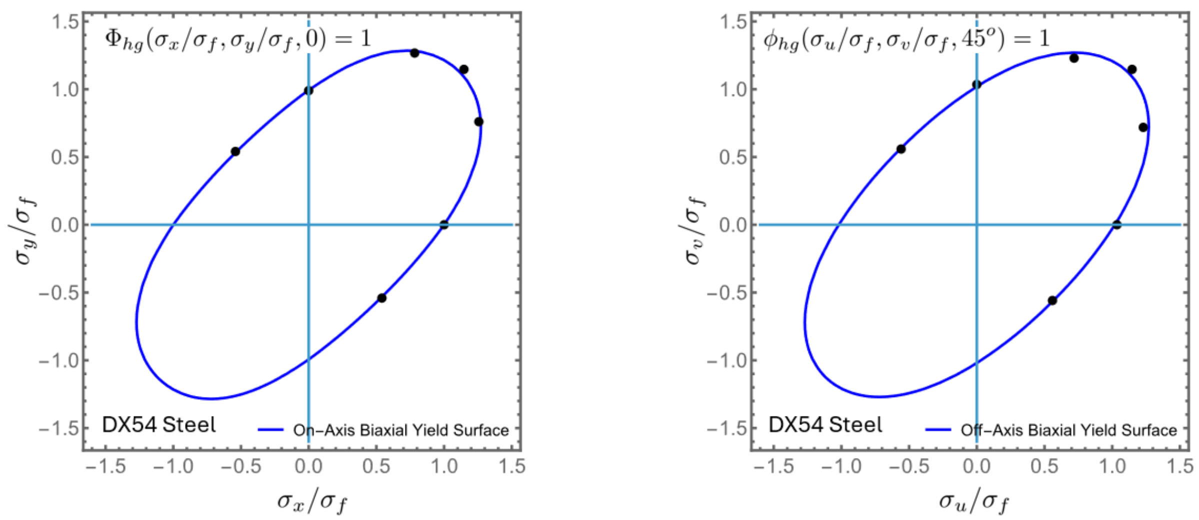

(a) (b)

Fig. 5. Predicted strictly convex (a) on-axis and (b) 45-degree off-axis biaxial yield surface contours by the sixth-order Hill–Gotoh yield function for DX54 steel sheet based on SOS-convexity constraints [3].

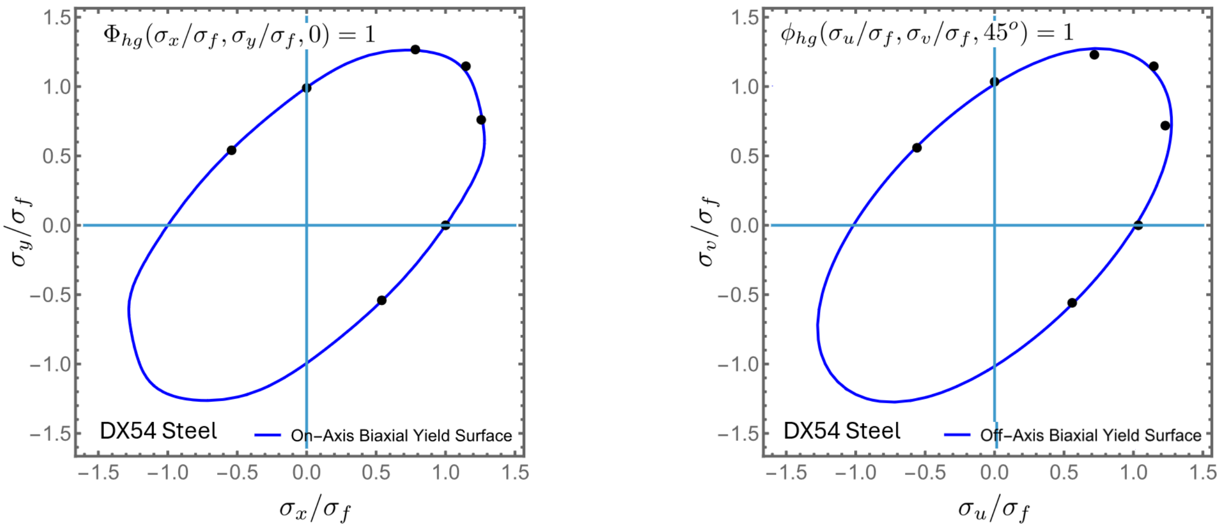

(a) (b)

Fig. 6. Predicted strictly convex (a) on-axis and (b) 45-degree off-axis biaxial yield surface contours by the sixth-order Hill–Gotoh yield function for DX54 steel sheet based on positive surface curvature constraints [10].

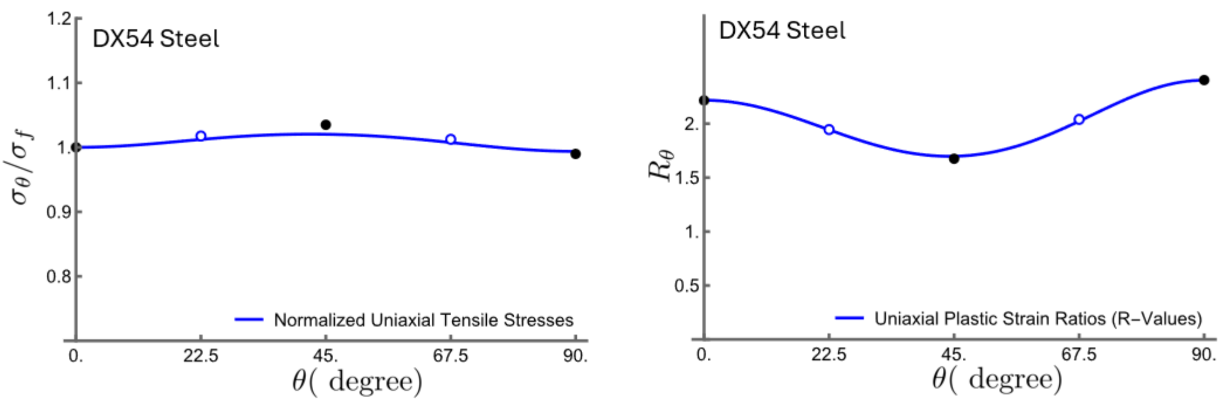

(a) (b)

Fig. 7. Predicted (a) uniaxial tensile yield stresses and (b) uniaxial tensile plastic strain ratios by the SOS-convex sixth-order Hill–Gotoh yield function for DX54 steel sheet [3,9]. Solid circles are experimental inputs while open circles are auxiliary inputs.

Summary

By extending to non-homogenous polynomials higher than fourth-order and by employing a least-square parameter identification method with novel convexity-constraints, the new numerical results of anisotropic yielding and plastic flow behaviors of three representative sheet metals show that the modeling capabilities of Hill-Gotoh theory can be extended to accommodate many more off-axis uniaxial and/or biaxial stress states of sheet metals with expanded convexity domains and improved accuracies.

References

[1] R. Hill, A theory of the yielding and plastic flow of anisotropic metals, Proceedings of the Royal Society of London, Series A. Mathematical and Physical Sciences, 193 (1948) 281-297.

[2] M. Gotoh, A theory of plastic anisotropy based on a yield function of fourth order (plane stress state)–I, International Journal of Mechanical Science 19 (1977) 505–12.

[3] W. Tong, A Hill–Gotoh theory of anisotropic sheet metal plasticity, International Journal of Mechanical Science 302 (2025) 110513. https://doi.org/10.1016/j.ijmecsci.2025.110513

[4] R. Hill, The Mathematical Theory of Plasticity. Clarendon Press, Oxford, 1950.

[5] F. Barlat, J.C. Brem, J.W. Yoon, K. Chung, R.E. Dick, D.J. Lege, F. Pourboghrat, S.-H. Choi, E. Chu, Plane stress yield function for aluminum alloy sheets Part 1: Theory, International Journal of Plasticity 19:9 (2003) 1297-1319.

[6] F. Barlat, H. Aretz, J. W. Yoon, M. E. Karabin, J. C. Brem, R. E. Dick, Linear transformation based anisotropic yield function, International Journal of Plasticity 21:5 (2005) 1009-1039.

[7] W. Tong, Algebraic convexity conditions for Gotoh's non-quadratic yield function, ASME Journal of Applied Mechanics 85 (2018) 074501-1

[8] H. Vegter, A.H. van den Boogaard, A plane stress yield function for anisotropic sheet material by interpolation of biaxial stress states, International Journal of Plasticity 22 (2006) 557-580.

[9] H. Vegter, M. Abspoel, J. Mulder, A plane stress yield surface using Bézier curve interpolation in two directions, IOP Conference Series: Materials Science and Engineering 651 (2019) 012052.

[10] W. Tong, An anisotropic plasticity theory of sheet metals based on a polynomial of Hill's 1948 yield function, International Journal of Solids and Structures 325 (2026) 113726. https://doi.org/10.1016/j.ijsolstr.2025.113726

[11] S. Boyd, L. Vandenberghe, Convex Optimization. Cambridge University Press, Cambridge, UK, 2004.

[12] V.A. Toponogov, Differential Geometry of Curves and Surfaces. Birkhauser (Boston), 2006.

[13] G. Reißig, Convexity of reachable sets of nonlinear ordinary differential equations, Autom. Remote Control 68:9 (2007) 1527–1543.

[14] J.W. Helton, J. Nie, Semidefinite representation of convex sets, Math. Program. Ser. A 122 (2010) 21–64.

[15] D. Henrion, C. Louembet, Convex inner approximations of nonconvex semial-gebraic sets applied to fixed-order controller design, International Journal of Control 85:8 (2012) 1083–1092.

[16] R. Goldman, Curvature formulas for implicit curves and surfaces, Comput. Aided Geom. Design 22 (2005) 632–658.